CONFERENCE PRE-PRINT

PHYSICS BASIS OF DISCREPANCIES BETWEEN TEMPERATURE MEASUREMENTS BY ECE AND THOMSON SCATTERING IN HIGH PERFORMANCE PLASMAS ON JET, EAST AND DIII-D

F.P. ORSITTO[1,3], L SENNI[3], G GIRUZZI[2], D MAZON[2], S MAZZI[2], M AUSTIN[4], F GLASS[5], SUK-HO HONG[5], TAEYEONG AN[14] , Y LI[6], Q ZANG[6], J LIU[6], M BASSAN[7], I WYSS[8], P GAUDIO[8] , O FORD[9], S ZOLETNIK[10], D KOS[11], M MASLOV[11], C CHALLIS[11], D FRIGIONE[8], L GARZOTTI[11], J HOBIRK[12] , A KAPPATOU[12], D KEELING[11], E LERCHE[13], C MAGGI[11], J MAILLOUX[11], F RIMINI[11], D VAN EESTER[13], JET CONTRIBUTORS[15] AND WPTE TEAM[16]

[1] ENEA Nuclear Department , C R Frascati , Via E Fermi 45 , 00044 Frascati , Italy
[2] CEA, IRFM, F-13108 Saint Paul-lez-Durance, France
[3] Istituto per le Applicazioni del Calcolo 'Mauro Picone' Consiglio Nazionale delle Ricerche (CNR), 00185 Rome, Italy
[4] Institute for Fusion Studies, Department of Physics, University of Texas at Austin, Austin, Texas 78712, USA
[5] General Atomics San Diego, CA 92121, United States of America
[6] Institute of Plasma Physics, Chinese Academy of Science, PO Box1126, Hefei, Hanui, People's Republic of China
[7] ITER IO, Route de Vinon, CS 90046,13067 Saint Paul Lez Durance, France
[8] Department of Industrial Engineering, University of Roma 'Tor Vergata', via del Politecnico 1, Roma, Italy
[9] Max-Planck-Institute fur Plasmaphysics, Greiswald, 17491, Germany
[10] Wigner Research Centre for Physics, Budapest, Hungary
[11] UKAEA, Culham Campus, Abingdon, Oxfordshire, OX14 3DB, UK
[12] Max-Planck-Institute fur Plasmaphysics, Boltzmannstr. 2, 85748 Garching, Germany
[13] Laboratory for Plasma Physics LPP-ERM/KMS, B-1000 Brussels, Belgium
[14] Division of Advanced Nuclear Engineering, Pohang University of Science and Technology, Pohang 37673, Korea
[15] See C.F. Maggi *et al.*, *Nucl. Fusion* **64**, 112012 (2024)
[16] See E. Joffrin *et al.*, *Nucl. Fusion* **64**, 112019 (2024)

*Corresponding author:*francesco.orsitto@enea.it

Abstract

Discrepancies between the Electron Cyclotron Emission (T_ECE) and Thomson Scattering (T_TS) measurements of electron temperature were observed on JET,TFTR , and more recently on FTU. This paper reports on the most recent study on this discrepancy conducted , in the context of ITPA Joint Activity on 'High Temperature Measurements', on JET DT3 (Third Deuterium-Tritium Campaign) , EAST and DIII-D. Models link these differences to the interaction of the heating systems with the electrons and then to the non-maxwellian nature of the electron velocity distribution function (EDF). Studying these effects is important for ITER and the fusion reactor where they can increase significantly. Studying these discrepancies, systematic effects and volume average related to different line of sights used for collecting the light must be taken into account. The discrepancies are detected on JET using two systems, i.e. HRTS (High Resolution Thomson Scattering) and LIDAR TS , on EAST and DIII-D. The consistency of these discrepancies across multiple diagnostics and machines rules out systematic effects as the underlying cause. On JET in Tritium rich scenario at Te=12keV there is a difference of ECE with respect to TS of the order of 25%, being T_ECE lower than T_TS. An empirical model of non-maxwellian bipolar perturbation fits the JET DTE3 database. Investigations started on EAST to see how the discharge conditions influence the EDF, and how combination of heating affects the ECE/TS discrepancy. The experiments were made in dominant ECRH heating with variation of plasma conditions and heating systems. In presence of Ion cyclotron heating T_TS>T_ECE was detected : the effect of fast ions on EDF could be considered in this scenario. Databases are collected on DIII-D to document the measurements of temperatures. The heating systems used on DIII-D are ECRH (Electron Cyclotron Resonance Heating), NBI (Neutral Beam Injection) and LH (Lower Hybrid) and discharges with combination of these systems are available. Systematic effect where T_ECE>T_TS for Te>7keV are reported , however this difference remain below the line of +10% difference.

1. INTRODUCTION

Discrepancies between the Electron Cyclotron Emission (T_ECE) and Thomson Scattering (T_TS) measurements of electron temperature were observed in plasmas heated by ECRH only (on FTU [1]) and NBI (JET[2],TFTR [3]) or NBI plus ICRH (on JET). Models link these differences to the interaction of the heating systems with the electrons and then to the non-maxwellian nature of the electron velocity distribution function (EDF) [4,5]. Studying these effects is important for ITER and the fusion reactor : while the presently detected differences can be of the order of 10-20% , they can increase significantly [5] for reactor plasmas where temperature can be of the order of 30-50 keV. The need of defining the measurement of the electron temperature precisely is of the highest relevance. Being so fundamental these themes are not new : the discussion started 30 years ago [3]. The radiation temperature T_r measured by the ECE diagnostic systems can be extracted from the Kirchhoff theorem [6] linking T_r to EDF and single electron emissivity $\boldsymbol{\eta_\omega}$:

$$k\,T_r = -\frac{\int \eta_\omega(p) f(p) d^3p}{\int \eta_\omega(p)(\partial f(p)/\partial\varepsilon) d^3p} = \frac{8\pi^3 c^2}{\omega^2}\frac{\beta_\omega}{\alpha_\omega}; \quad S_\omega = \frac{\omega^2}{8\pi^3 c^2} k\,T_r \qquad (1)$$

where f(p) is the EDF (p electron momentum) and ε is the electron energy, β_ω is the plasma emissivity and α_ω the absorbtion coefficient .The radiation flux S_ω is the flux of photons emitted by electrons in the plasma and it is expressed by the Rayleigh-Jeans formula. Therefore for maxwellian electrons T_r is equal to the electron temperature, as it can be verified using eq.(1). Since the absorbtion coefficient depends on the derivative of the EDF with respect to energy (see eq.(1)) , T_{rad} is sensible to distrortions of EDF, i.e. to non-maxwellian nature of EDF. The signal measured by the ECE diagnostics must take into account an integration along a line of sight of the photons transported through the plasma. So using the equation of radiation transfer [6] the radiation temperature detected can be expressed by the following expression [7]:

$$T_{rad}(\omega) = \int_{R_0-a}^{R_0+a} F_{rad}(R)\,dR = \int_{R_0-a}^{R_0+a} \beta_\omega(R)\left[\exp\left(-\int_R^{R_0+a} \alpha_\omega(R')\,dR'\right)\right] dR \qquad (2)$$

where R_0 (a) is the torus major (minor) radius. The evaluation of the F_{rad} for the 2nd harmonic extraordinary mode emitted by the plasma for electron temperatures Te=1,5,10keV shows that increasing the electron temperature the peak of Frad decreases toward low electron energies: for example for Te=10keV the Frad peaks at E/Te=0.5 (Fig.1a) , the radiation temperature then samples low energy electrons. This tendency is reversed at low temperatures : Frad peaks for electron energies close to the electron temperature (see Fig.1b).

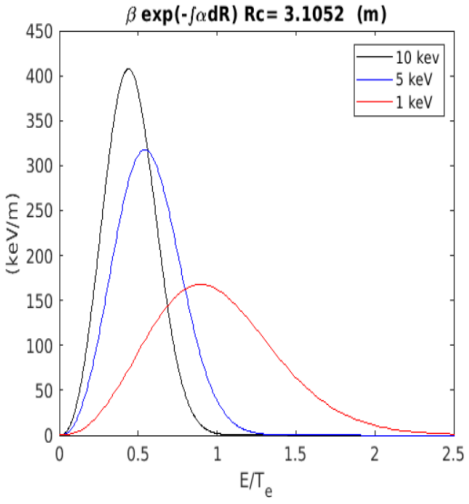

Fig.1a. Frad vs E/Te for Te=1,5,10keV

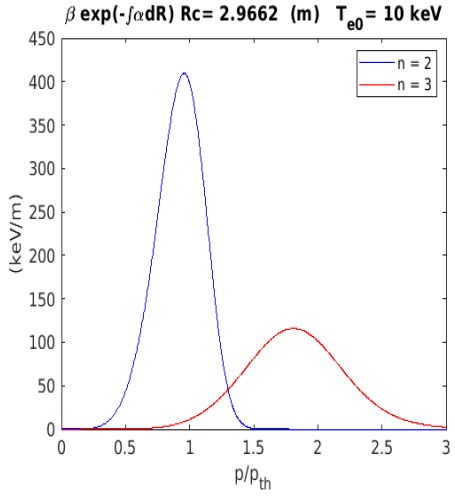

Fig.1b Frad vs E/Te for the 2nd and 3rd Harmonic Xmode

The Fig.1b shows the range of electron energies where the Frad is sensitive related to the 2nd and 3rd harmonic X-mode at Te=10keV : the 2nd harmonic corresponds to electron energies of the order of the electron temperature , whole the 3rd harmonic covers a range of electron energies higher than the electron temperatures .

So the two harmonics probe different parts of the electron energy distribution function. In Fig.1a and b the value of R_c corresponds to the actual value of R_0 in (2). Moving to the Thomson scattering (TS) spectrum , it is worth noting that the spectrum of the scattered light $P_{TS}(\omega)$ is proportional to the electron velocity distribution function where the frequency shift with respect to the laser frequency is corresponding to the Doppler shift of the radiation emitted by the electrons [8] :

$$P_{TS}(\omega) \propto \int f(\vec{v})\, \delta(\vec{k}.\vec{v}-\omega)\, d\vec{v} \qquad (3)$$

where f(v) is the EDF, k = ki-ks is the difference between the wavevectors of the incident light (ki) and scattered light (kf). The eq. (3) is a very simplified expression which is not taking into account polarization effects which are important for relativistic electrons. In principle the TS is measuring the EDF in a geometry defined by the k-wavevector.

2. THE MEASUREMENT OF ELECTRON TEMPERATURE : SYSTEMATIC AND STATISTICAL ERRORS , LINE OF SIGHTS AND VOLUME AVERAGES.

In the process of comparing the measurements of Te made by ECE and TS, systematic effects and volume average related to different line of sights used for collecting the light must be taken into account. For the comparison ECE/TS on JET , the ECE Martin-Puplett interferometer (MPI) [9] is usually taken (system JET-KK1) and the measurements of LIDAR TS [10] and HRTS [11,12] (High resolution Thomson Scattering , system JET-K11) are used. In ECE and TS the measurement is done collecting light along specific line of sights and the signal is averaged on different plasma volumes. A meaningful comparison between these two diagnostics must account for differences in lines of sight, sampled volumes, and temporal resolution. As detailed in [13], the comparison is carried out over nearly identical volumes at each time instant.The dimensions (vertical/z and horizontal/radial, in the poloidal plane) of the volumes where the two diagnostics acquire signals are approximable with cylinders of dimensions as reported in Table I. Averaging over a region with a radial extension of 15 cm (5-6 measurement points) allows to compensate for the different spatial resolutions and measurement volumes of the two systems, and using the same flux coordinates ensures that both diagnostics refer to the same plasma region, despite their different lines of sights. The Fig.2a (left) shows the line of sights of instruments used at JET for the measurements of electron temperature reported in this paper: light blue line describes the line of sight of the ECE Martin-Puplett (MPI) interferometer, the red line the HRTS: the distance between them is of 5-6cm . It is very important to note that the measurements of ECE MPI and HRTS are averaged over the same flux coordinates range, as shown in fig.2b-right, where the approximate averaging volumes of both diagnostics, mapped to the same flux-coordinate interval are highlited in blue and violet.

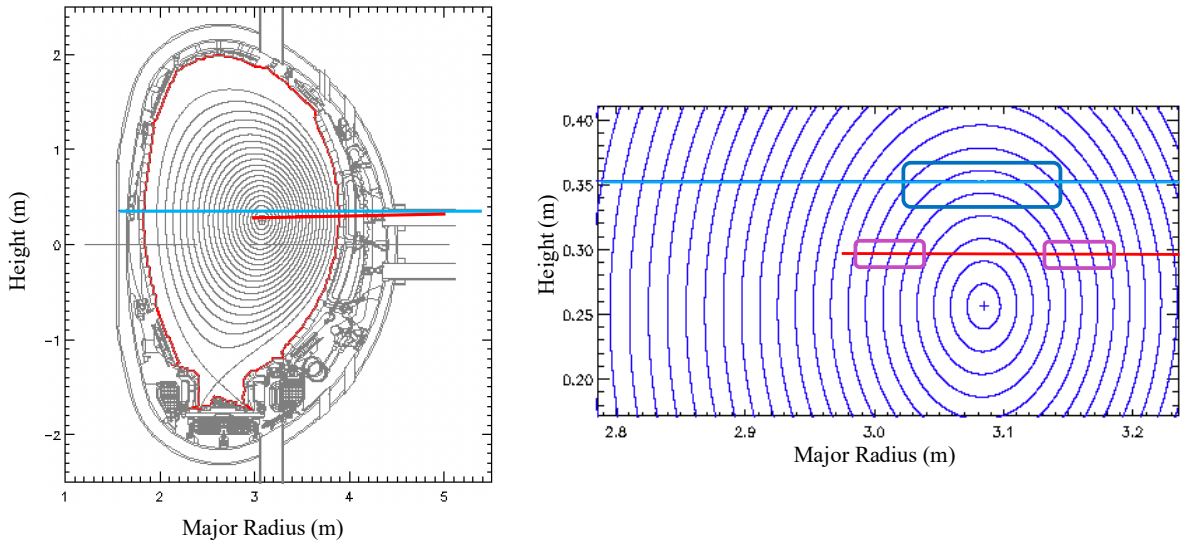

FIG.2a (left) :Line of sights of the JET systems, light blue ECE Martin-Puplett interferometer(MPI), red HRTS . Fig.2b(right): the volumes covered by HRTS (violet) and MPI (blue) corresponding to the same flux coordinate.

Another fundamental aspect of the ECE/TS comparison is the assessment of statistical and systematic errors affecting the instruments HRTS and MPI, so it is useful to note that :

i) during the DTE3 campaigns ECE calibration checks were carried out weekly

ii) the spectral calibration of HRTS affecting the evaluation of temperature was re-checked for DTE3 campaign

iii) the evaluation of systematic errors is difficult: the checks on the hardware can reduce them. On the other side, the discrepancies between ECE and TS were detected using two systems, i.e. HRTS[12] and LIDAR TS[7] on JET , and on EAST, DIII-D and preliminarly also on W7X. The variety of the devices excludes systematic effects on their evaluation. The consistency of these discrepancies across multiple diagnostics and machines rules out systematic effects as the underlying cause.

iv) The error bar on the measurements of TS is of the order or less than 5%, since it results from average of at least two experimental points .

v) The evaluated error bar on the ECE MPI measurements is < 5%

TABLE I	Radial extension mm	Vertical extension mm
ECE MPI	28	36
HRTS	16	22

Table I . Dimensions of the measurements volumes for ECE and TS on JET

3. COMPARISON OF TEMPERATURES MEASURED BY ECE and TS ON JET DTE3 campaign.

About 475 pulses were selected for the analysis , the global comparison is presented in Fig.3. Given the large number of data points, a density plot is used to highlight the general trend, representing how the experimental points are distributed by indicating how many falls within different regions of the plane.

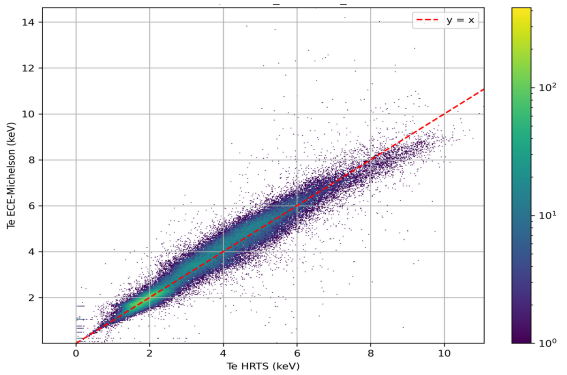

Fig.3 T_ECE vs T_HRTS: DTE3 campaign.

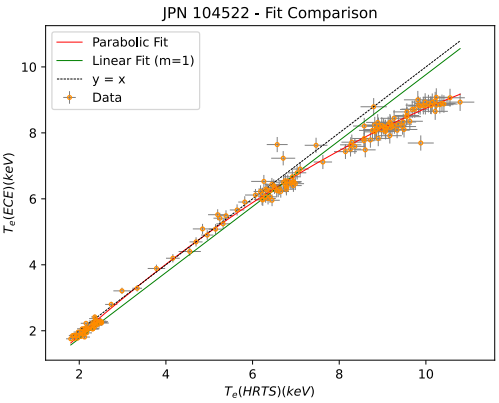

Fig.4 . T_ECE vs T_HRTS for the pulse#104522.

Note that the temperatures shown are averaged over the plasma center (approximately 15 cm) and are therefore slightly lower than the peak temperatures. Systematically the T_ECE < T_HRTS for Te>7keV. The difference T_HRTS – T_ECE= 1-1.5 keV at Te_HRTS=9keV. Figure 4 shows T_ECE versus T_HRTS for the fusion record DTE3 pulse#104522: fits (linear/green line and quadratic/red line) to the data are indicated in the plot and the error bars are shown on each point. The quadratic trend agrees very well with the model presented in Fig. 6. The T_ECE=T_HRTS for Te< 7keV , but a feature of the plot in Fig.4 is that above the T_HRTS >10keV a saturation of the T_ECE is observed (the difference between ECE and TS increases) . Modelling the ECE/TS discrepancy using a bipolar model [9] of non-maxwellian electron velocity distribution function is very useful for demonstrating in a particular case how the non-maxwellian nature of EDF can affect the ECE/TS discrepancy. The Fig.5 shows the maxwellian EDF (f_M, blue line) wih the bipolar perturbation (f_1, red line), the region of EDF corresponding to 2nd and 3rd harmonic X-mode measurements are also shown. The parameters defining f_M and f_1 non-maxwellian perturbation are given in the following eq.:

$$f = f_M + f_1;\ f_M = A\exp(-\mu(\gamma-1));\ f_1 = f_0\sin\left(\frac{(p-p_0)}{\delta_0}\right);\ \mu = \frac{m_e c^2}{T_e};$$
$$\gamma = (1-(v/c)^2)^{-1/2};\ A = \mu\exp(-\mu/4)\ K_2(\mu);\ p_{th} = m_e v_{th} = m_e\left(\frac{T_e}{m_e}\right)^{1/2} \quad (4)$$

The Fig.6 shows the evaluation of the radiation temperature measured by the ECE diagnostic system over the a database of DTE3 which includes all the record pulses of the tritium rich scenario [14]: data-measurements (2nd harmonic X-mode) are represented by light blue , theoretical evaluation in dark blue. The figure shows that at Te=12keV there is a difference of ECE with respect to TS of the order of 25%, being T_ECE lower than T_TS . It is really a nice feature that the bipolar perturbation (see Fig.6 top title) fits the database with the following parameters : p_0/p_{th}=1.5, δ_0/p_{th}=0.7, f_0=0.05 , and the wall reflection coefficient used in the evaluation is Ref=0.55. The message of the Fig.6 is that a small perturbation (f_0=5%) of the maxwellian EDF, positioned in the high velocity side of the EDF (v_0/v_{th}=1.5) , quite wide in the velocity space δv/vth =50% can produce a substantial effect on ECE radiation temperature of the ECE 2nd harmonic X-mode. The evaluation at highest temperature (Te>10keV) shows a small under-evaluation of the ECE/TS discrepancy by the theoretical bipolar model.

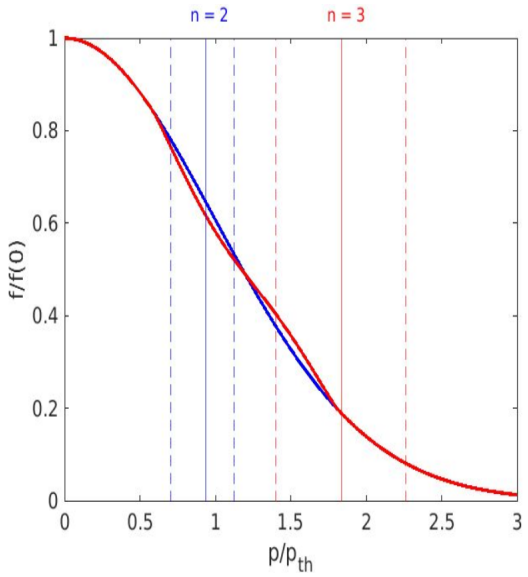

Fig .5 Bipolar perturbation on a Maxwellian EDF

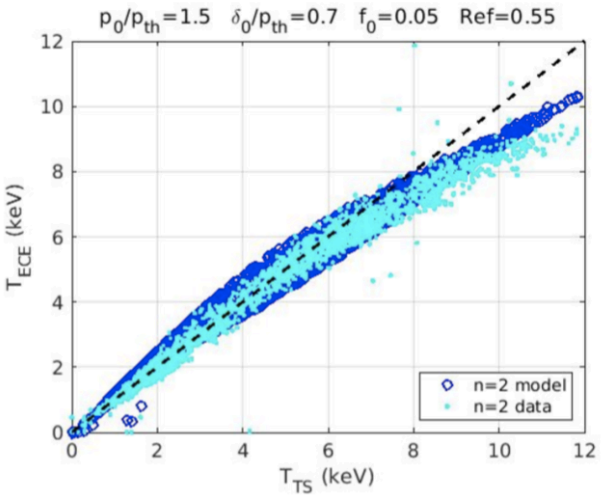

Fig.6 Evaluation of T_ECE using Bipolar EDF

This slight under-evaluation suggests that something is missing in the model, which was not the case for the discharges presented in [7], most of which were in Deuterium. In fact, the discharges of the DTE3 campaign that reach the highest temperature values at high density have a significant contribution of heating by the alpha particles, increasing as T^2 as the DT fusion cross section. Assuming that the intensity of the bipolar perturbation increases as T^2 the agreement between data and model improves significantly. An additional challenge is found if we try to match data and model for both the 2nd and the 3rd harmonic, i.e., in the two different velocity ranges seen by the two harmonics. To this end, the model can be further complexified in two ways:

1) Still using sinusoidal perturbations, but not bipolar
2) Combining two perturbations acting in two different velocity ranges.

Using this type of model, a satisfactory agreement is found for the full DTE3 data base (> 5000 data points) for both harmonics, as shown in Fig. 7a. The perturbed distribution function (shown in Fig. 7b) has still rather small distortions with respect to the Maxwellian. Of course, much better agreement could be obtained for selected group of discharges with homogeneous physical properties. The physical nature of the mechanisms causing such perturbations has still to be fully unveiled. It can be related to the three heating systems (alpha, NBI, ICRH) and/or to MHD instabilities.

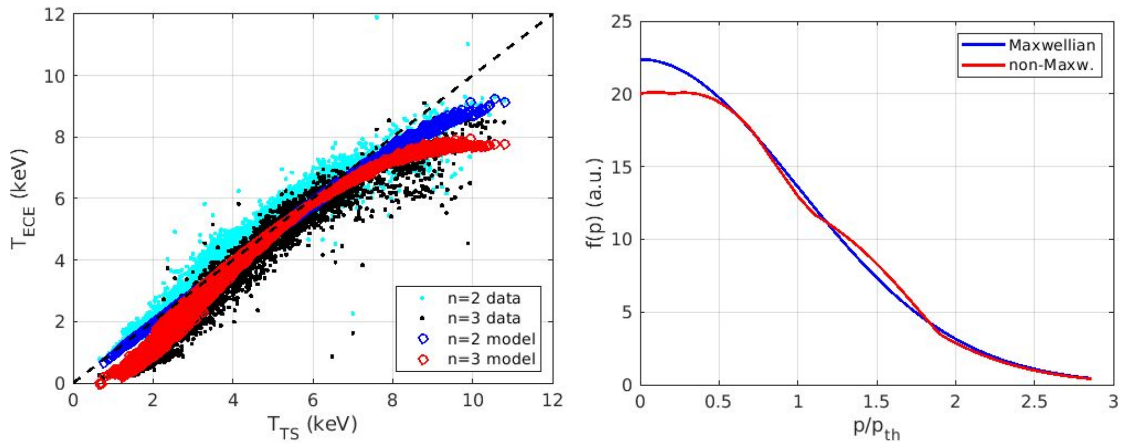

Fig. 7a(left): Central electron temperature measured by ECE (MPI) vs the same quantity measured by Thomson scattering (HRTS). Measured data are shown together with data computed using the perturbed EDF shown in at right. Fig.7b(right): Maxwellian (blue) and perturbed (red) EDF, using the model with two non-bipolar perturbations.

4.MEASUREMENTS OF ECE AND TS DISCREPANCIES ON EAST TOKAMAK

The physics basis of the discrepancy between ECE and TS electron temperature measurements is discussed in sec.1. The interaction of heating systems (ECRH , NBI , ICRH heating and generated fast ions , alpha particle heating in DT plasmas) with plasma electrons could lead to a distortion of the electron EDF. The effects of collisional relaxation of fast ions on electron distribution function were evaluated in ref [15] in a case study of the alpha particle effects on EDF : the solution of Focker-Planck equation led to a bipolar EDF. A study of EC-heating on electrons made in [4] revealed effects on EDF in the context of evaluation of differences of electron temperatures between ECE and TS. Fast ion dominated discharges presumably produce effects on EDF different from RF dominated electron heating. Starting from this point an experiment started on EAST to investigate how the discharge conditions influence the EDF , and also in this context how the combination of various heating affects the differences between ECE and TS measurements. These experiments were made in dominant ECRH heating with variation of plasma conditions and heating systems Under Li-wall conditioning Thomson electron temperature measurements were higher than ECE i.e. T_TS>T_ECE. While in conditions of B-wall conditioning no effects were detected on ECE / TS measuremnts. In presence of Ion cyclotron heating T_TS>T_ECE was detected : the effect of fast ions on EDF could be considered in this scenario. The preliminary summary of the results obtained on EAST is reported in Fig.7 where each experimental point is resulting from different combination of heating.

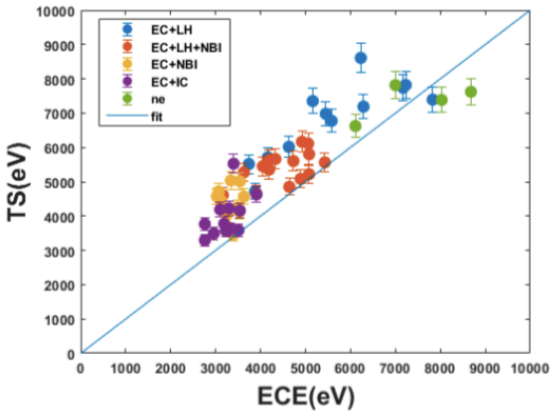

Fig.7 EAST : ECE vs TS measurements with various heatings and plasma conditions

Looking into the Fig.7 , in general all the various combinations of heating produce differences between ECE and TS . In practically all cases T_TS >T_ECE , the opposite (T_ECE>T_TS) happens for neon seeded discharges and for one case of EC-LH heating. The maximum difference between ECE and TS is reached in discharges

EC-LH (Electron cyclotron combined with lower hybrid heating) : this is a condition of pure electron heating. Strong effects are obtained also combining ECRH with NBI and ICRH where the fast ions play a fundamental role on EDF structure changes. The analysis of these results is ongoing.

4.MEASUREMENTS OF ECE versus TS DISCREPANCIES ON DIII-D TOKAMAK.

Databases are collected on DIII-D tokamak to document the measurements of temperatures by ECE and TS. The heating systems used on DIII-D are ECRH , NBI and LH and discharges with combination of these systems are available. The 'Tangential' TS (TTS) system is providing temperatures on the plasma centre , while the ECE radiometer the measurements across the full plasma region : Fig.8 shows the relative positions of the ECE radiometer and TTS in the poloidal plane together with the equilibrium surfaces.

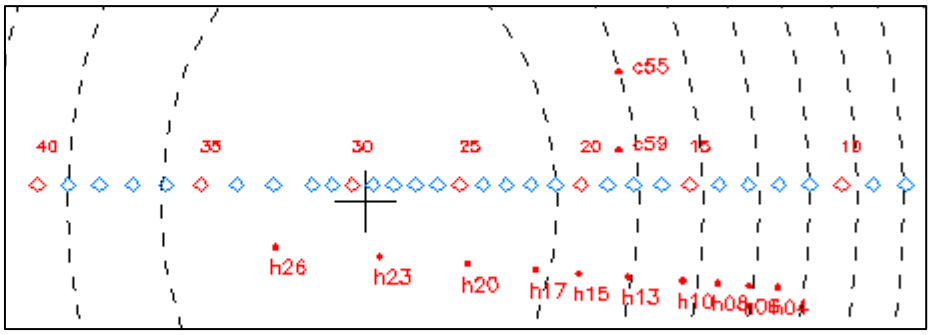

Fig.8 positions of TTS (red points) and ECE radiometer (red and blue diamonds) at t=3100ms pulse#191947

For the pulse #191947 the ECE vs TTS temperature profiles are given in fig.9.

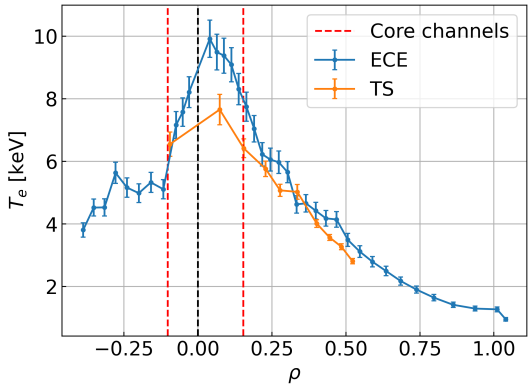

Fig.9 ECE and TTS profiles, pulse #191755 .

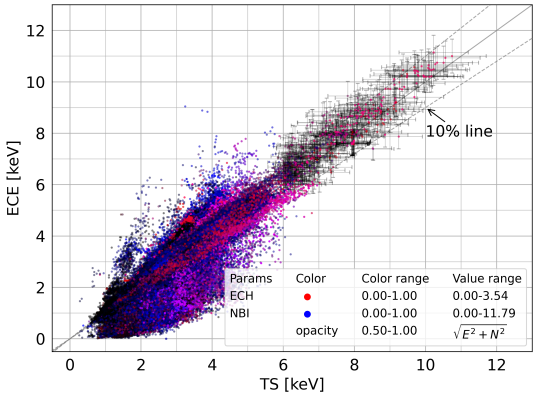

Fig.10 ECE vs TTS DIIID database .

The difference T_ECE - T_TTS≈+2keV is at plasma centre for the pulse#191755. In general the ECE vs TTS comparison on the complete DIII-D database is shown in Fig.10: the plot includes about 256443 points, with DIII-D pulse number <197000, the error bars are shown for the points with Te>6keV, the Thomson error bars are often >10%, the shots with ECRH and NBI are marked with different color and 10% difference lines are drawn. The Fig.10 shows a systematic effect where T_ECE>T_TTS for Te>7keV , this difference remain below the line of +10% difference. The algorithm used to construct the dataset is a prototype : it would need further optimization . In DIII-D yr 2025 campaign, a new database is available including 170 pulses: LH heated pulses with high temperatures as well as H-mode with NBI-ECRH heating are available , the analysis is ongoing.

ACKNOWLEDGEMENTS

The authors are grateful to ITPA TG Diagnostics and the ENEA Nuclear Department for the interest in the work reported in this paper. The corresponding author is grateful to IAEA for providing support for the participation to the IAEA FEC25.Work supported by US DOE under DE-FC02-04ER54698 and DE-FG02-97ER54415. Disclaimer: This report was prepared as an account of work sponsored by an agency of the United States

Government. Neither the United States Government nor any agency thereof, nor any of their employees, makes any warranty, express or implied, or assumes any legal liability or responsibility for the accuracy, completeness, or usefulness of any information, apparatus, product, or process disclosed, or represents that its use would not infringe privately owned rights. Reference herein to any specific commercial product, process, or service by trade name, trademark, manufacturer, or otherwise does not necessarily constitute or imply its endorsement, recommendation, or favoring by the United States Government or any agency thereof. The views and opinions of authors expressed herein do not necessarily state or reflect those of the United States Government or any agency thereof.

REFERENCES

1. G Pucella et al, 'Overview of FTU Results', Nucl Fusion 62(2022)042004
2. E. de la Luna, V. Krivenski, G. Giruzzi, C. Gowers, R. Prentice, J. M. Travere, and M. Zerbini, "Impact of bulk non-Maxwellian electrons on electron temper- ature measurements," Rev. Sci. Instrum. 74(3), 1414–1420 (2003).
3. G. Taylor, E. Fredrickson, B. Grek, and A. Janos, 'Electron Cyclotron Emission Measurements on High [Beta] TFTR Plasmas' (World Scientific Publishing Co. Pte. Ltd., Borrego Springs, CA, 1995).
4. V Krivenski, 'Electron cyclotron emission by non-Maxwellian bulk distribution functions' Fusion Eng. Des. 53(1), 23–33 (2001)
5. G Giruzzi , 'A model of non-Maxwellian electron distribution for the analysis of ECE in JET discharges', EC-21 paper 67 and IAEA FEC London 2023, CN 125/45.
6. G Bekefi , 'Radiation Processes in Plasmas', J Wiley 1966, sec.2.3. eq.2.47.
7. M Fontana et al , 'Investigation of Te measurements discrepancies between ECE and Thomson diagnostics in high-performance plasmas in JET', Phys. Plasmas 30, 122503 (2023) .
8. D H Froula , S H Glenzer , N C Loumann Jr, J Sheffield , 'Plasma Scattering of Electromagnetic Radiation', Elsevoer 2011.
9. S. Schmuck, J. Fessey, J. E. Boom, L. Meneses, P. Abreu, E. Belonohy, and I. Lupelli, "Electron cyclotron emission spectra in X- and O-mode polarisation at JET: Martin-Puplett interferometer, absolute calibration, revised uncertainties, inboard/outboard temperature profile, and wall properties," Rev. Sci. Instrum. 87(9), 093506 (2016).
10. H. Salzmann, J. Bundgaard, A. Gadd, C. Gowers, K. B. Hansen, K. Hirsch, P. Nielsen, K. Reed, C. Schr€odter, and K. Weisberg, "The LIDAR Thomson scat- tering diagnostic on JET (invited)," Rev. Sci. Instrum. 59(8), 1451–1456 (1988)
11. R. Pasqualotto, P. Nielsen, C. Gowers, M. Beurskens, M. Kempenaars, T. Carlstrom, and D. Johnson, "High resolution Thomson scattering for Joint European Torus (JET)," Rev. Sci. Instrum. 75(10), 3891–3893 (2004)
12. F. P. Orsitto et al, Study on Differences of ECE and High Resolution Thomson Scattering temperature measurements in DT(Deuterium-Tritium) plasmas on JET, EPS 23 Bordeaux Paper Mo_MCF #1.019(2023)
13. L. Senni, F.P. Orsitto, M. Fontana, S. Mazzi, E. Giovannozzi, G. Giruzzi,'Standardizing High Electron Temperature Measurement Comparisons: A Method for Cross-Diagnostic and Cross-Machine Analysis' JINST 20(2025) C09009,https://doi.org/10.1088/1748-0221/20/09/C09009
14. M. Maslov et al, 'JET D-T scenario with optimized non-thermal fusion', 2023 Nucl. Fusion 63 112002
15. B Appelbe et al., 'Modification of classical electron transport due to collisions beween electrons and fast ions', Phys Plasmas 26(2019) 102704.